Fluctuations in catalytic surface reactions

2003 New J. Phys. 5 62

(http://iopscience.iop.org/1367-2630/5/1/362)

New Journal of Physics
An Institute of Physics and Deutsche Physikalische Gesellschaft Journal

Fluctuations in catalytic surface reactions

R Imbihl
Institut für Physikalische Chemie und Elektrochemie, Universität Hannover, Callinstraße 3-3a, D-30167 Hannover, Germany
E-mail: imbihl@pci.uni-hannover.de

New Journal of Physics **5** (2003) 62.1–62.17 (http://www.njp.org/)
Received 5 February 2003
Published 6 June 2003

Abstract. The internal reaction-induced fluctuations which occur in catalytic CO oxidation on a Pt field emitter tip have been studied using field electron microscopy (FEM) as a spatially resolving method. The structurally heterogeneous Pt tip consists of facets of different orientations with nanoscale dimensions. The FEM resolution of roughly 2 nm corresponds to a few hundred reacting adsorbed particles whose variations in the density are imaged as brightness fluctuations. In the bistable range of the reaction one finds fluctuation-induced transitions between the two stable branches of the reaction kinetics. The fluctuations exhibit a behaviour similar to that of an equilibrium phase transition, i.e. the amplitude diverges upon approaching the bifurcation point terminating the bistable range of the reaction. Simulations with a hybrid Monte Carlo/mean-field model reproduce the experimental observations. Fluctuations on different facets are typically uncorrelated but within a single facet a high degree of spatial coherence is found.

Contents

PII: S1367-2630(03)59263-1

1. Introduction

Due to the statistical nature of the elementary processes of reaction and diffusion fluctuations are always present in chemical reaction systems [1]–[8]. Since the relative amplitude of fluctuations in general scales like $(1/N)^{1/2}$ with N being the number of molecules, the influence of fluctuations can only become prominent for very small systems. If this is the case, one may observe a departure from behaviour predicted by macroscopic rate laws, i.e. one may, for example, find fluctuation-induced transitions in a bistable system. Macroscopic rate laws predict that the system resides on one of the two steady-state branches for an indefinite period of time.

Due to their importance in a number of fundamental questions fluctuations have received extensive theoretical treatment in numerous text books [1]–[6]. The small number of experimental studies contrasts the central role fluctuations play in theory. External noise has been investigated with optical, electrical and chemical systems [3, 6, 10]. In single-molecule spectroscopy intermittency was observed [9] but quite generally the role of internal noise or fluctuations in chemical reaction systems has scarcely been studied experimentally because well defined experiments with microscopic reaction systems are inherently difficult.

Small scale reaction systems where the influence of fluctuations is potentially large are nevertheless of great practical importance as demonstrated by the example of supported catalysts in heterogeneous catalysis [11]. Such catalysts, consisting of small metal particles of typically a few nanometres diameter on a ceramic support, represent the workhorse in real catalysis. With the design of nano-scale catalysts and nano-scale reaction systems, fluctuations became an issue for all scientists involved in the construction or analysis of such systems [12, 13]. Even without implementing them by design nano-scale systems form naturally on a catalytic surface due to attractive or repulsive forces between adsorbed particles. This represents of course a well known fact in surface science but fluctuations and stochastic events play a very important role in pattern formation in these systems as was demonstrated in a recent theoretical analysis [14].

An experimental technique that very conveniently allows the simultaneous observation of a few thousand reacting particles on a catalytic metal surface is field electron microscopy (FEM) [15]. The surface of a field emitter tip (FET) which can be imaged *in situ* with FEM with ≈20 Å resolution consists of small facets of similar extension as the metal particles of a supported catalyst. The FET can therefore be considered as a model system for a supported catalyst. The reaction system we chose to investigate is catalytic CO oxidation on platinum. This reaction system exhibits a variety of different chemical wave patterns and oscillatory kinetics studied extensively on different platinum single-crystal surfaces [16, 17]. FEM and field ion microscopy (FIM) have been applied to study oscillatory kinetics on Pt and Rh surfaces [18]–[20]. In our studies we focused entirely on reaction conditions under which the system $Pt/CO + O_2$ is bistable and therefore easier to analyse [21]–[26]. These studies, which are summarized in this report, demonstrate that FEM, which has almost completely been replaced in surface science laboratories by the scanning tunnelling microscope (STM), is in fact a technique with which fluctuations in catalytic reactions can be nicely investigated. This report is organized such that we first focus on the temporal behaviour of fluctuations before considering spatial correlations and coupling effects between neighbouring facets.

The experiments are complemented by Monte Carlo (MC) simulations, conducted by the group of Evans in Ames, USA, and by Pavlenko in Hannover and Munich [23, 25, 27]–[29]. The question of how to appropriately model catalytic reactions is by no means trivial due to the very different length and time scales involved. The general topic of fluctuation effects in finite bistable

reaction systems has been explored extensively at the so-called mean-field (MF) level using master equations, stochastic rate equations or associated Fokker–Planck equations [3, 4, 7, 28]. Given that rapid surface diffusion of mobile adsorbates on a catalytic surface ensures perfect mixing, the use of MF equations is certainly justified. In reality, however, some adsorbates may have an extremely low mobility and energetic interactions between the adparticles may lead to island formation and induce overlayers. Spatial correlations, which are thus generated, are completely neglected in the MF approach. These spatial correlations can, in principle, be treated exactly in atomistic lattice-gas models [29]. On the other hand, MC simulations cannot provide a realistic description of the fast CO diffusion because computational restrictions do not allow implementing a realistic hopping rate. The way out of this dilemma was the construction of a hybrid model combining MC simulations with an MF description [27]. This method was used for the simulation of the experimental FEM results.

2. Experimental methods and data analysis

2.1. Experimental methods

The principle of the experimental FEM set-up is rather simple as demonstrated by figure 1(A). By applying a high enough field between a FET and screen electrons are emitted from the tip and accelerated onto the screen [15]. Just by the geometrical projection atomic resolution can in principle be reached but with electrons the resolution is limited to about 20 Å. Only when the polarity is reversed and the field-induced ionization of noble gas atoms is used to image the tip can a resolution of ≈2–3 Å be reached with an instrument that is then operated as a field ion microscope (FIM) [15].

To a good approximation the shape of a FET can be represented by a hemisphere as shown by the ball model in figure 1(B). In principle, all surface orientations are present similar to a stereographic projection but only the low-index planes (111), (100), and (110) have dimensions of more than a few lattice constants. The edge atoms of the facets are represented as bright balls in figure 1(B). Only these atoms are imaged intensely in FIM because of the electric field strength, which varies as $1/r$. An FIM image of the (100)-oriented Pt tip used in our experiments is displayed in figure 1(C). The four (211) orientations, which are present due to the fourfold symmetry of the (100)-oriented tip, have been marked because later on we will compare their fluctuation behaviour. The enlarged view of the FIM image in figure 1(D) shows a (211) facet of 5.5 nm terminated by an atomic step with only the edge atoms of the facet being imaged brightly in FIM.

Under reaction conditions we use FEM and not FIM as the *in situ* method for studying the fluctuations because FEM operates with a lower field strength of ≈0.4 V Å^{-1} as compared to the 1.2–1.5 V Å^{-1} of FIM (O_2 as imaging gas). In contrast to FIM field-induced effects in catalytic CO oxidation are negligible in FEM as was demonstrated in measurements with on–off duty cycles [31]. The brightness in FEM varies with the local work function (WF). The CO-covered and bare surface (low WF) are therefore imaged as bright areas whereas the oxygen-covered surface (high WF) appears dark as shown by the FEM image in figure 1(E) [15, 21]. The magnification of both methods, FEM and FIM, is given by geometrical projection of the tip onto the screen and therefore practically identical. FIM with its high resolution of ≈3–4 Å can therefore be used to identify the precise crystallography of the surface region which is probed under reaction conditions with FEM with a much lower resolution of ≈20 Å. The FEM images

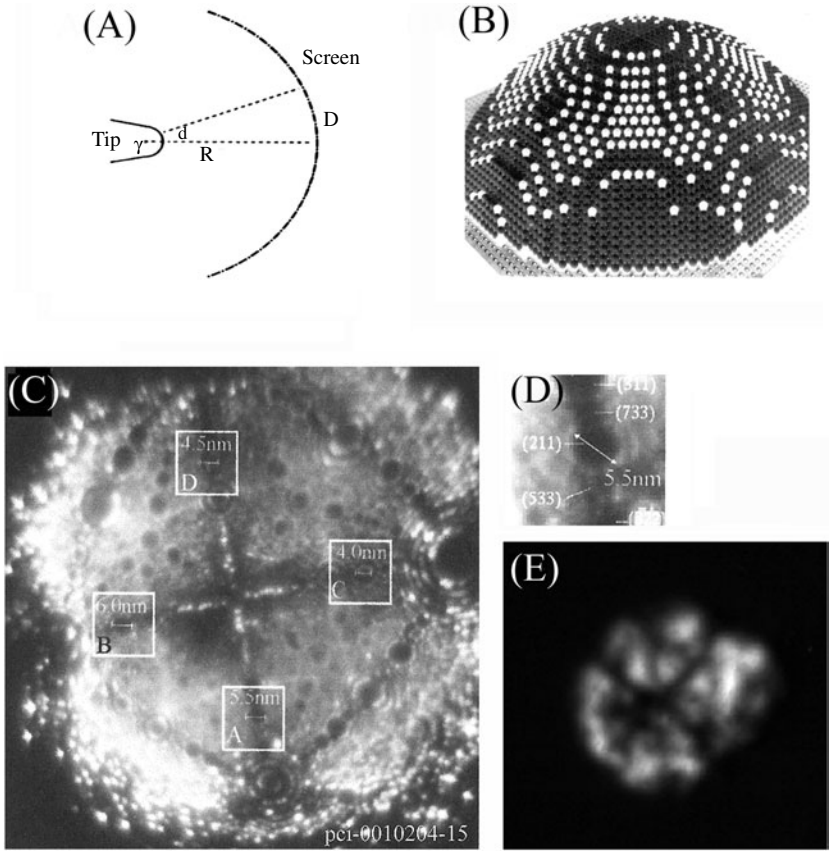

Figure 1. Catalytic CO oxidation on a Pt FET (from [23] and [26]). (A) Schematic experimental set-up for field electron and field ion microscopy. (B) Ball model of a FET (reproduced from [30]). (C) FIM image showing the crystallography of the [100]-oriented Pt tip. The four symmetry equivalent (112) orientations used in studies of fluctuations are marked. (D) Enlarged view of the Pt(211) facet in (C) showing atomic steps terminating the left and right edges of the facet. (E) FEM image of the Pt tip under reaction conditions ($T = 310$ K, $p_{O_2} = 4.0 \times 10^4$ Torr, $p_{CO} = 4 \times 10^{-7}$ Torr, field strength $F = 0.4$ V Å^{-1}).

are recorded with a video camera and digitized with 8 bit resolution. The temporal resolution with a conventional video camera is limited to 20 ms/frame.

2.2. *Data analysis*

The autocorrelation function $C_I(t)$ for fluctuations of the local intensity $I(t)$ is defined as

$$C_I(t) = \langle \delta I(t' + t) \delta I(t') \rangle_{t'} \tag{1}$$

where $\delta I(t) = I(t) - \langle I(t) \rangle$ is a brightness fluctuation at time t, and $\langle I(t) \rangle$ is the averaged local intensity.

The spatial correlation $C_I^{AB}(\boldsymbol{r}_A, \boldsymbol{r}_B)$ between fluctuations on region A and fluctuations on a second region B separated by d is defined by

$$C_I^{AB}(\boldsymbol{r}_A, \boldsymbol{r}_B) = \langle \delta^A I(t) \delta^A I(t) \rangle_t \tag{2}$$

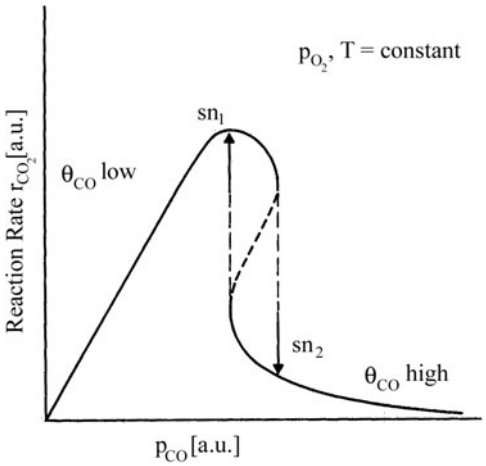

Figure 2. Schematic diagram showing the stationary branches of the reaction rate in the bistable $CO + O_2$ reaction on platinum.

with the average being performed over the time. Note that due to boundary effects the spatial correlation function depends on the positions $\boldsymbol{r}_A$ and $\boldsymbol{r}_B$ and not just on the spatial separation $d = |\boldsymbol{r}_A - \boldsymbol{r}_B|$, i.e. the correlation function is not translationally invariant.

With video sequences one has in principle the full spatiotemporal information of the dynamics of the reaction, but in order to utilize this information, effective methods of data reduction are required, and the method we employ here is the so-called Karhunen–Loeve decomposition (also known as proper orthogonal decomposition = POD) [32]. In POD the spatiotemporal signal $w(\boldsymbol{x}, t)$ is represented as a superposition of eigenimages or modes, $\Psi_n(\boldsymbol{x})$, where the dynamics are contained in the time-dependent coefficients $A_n(t)$:

$$w(\boldsymbol{x}, t) = \sum_{n=1}^{\infty} A_n(t)\Psi_n(\boldsymbol{x}). \tag{3}$$

Primarily, POD is a method of data reduction and noise filtering but applied to complex spatiotemporal dynamics the resulting modes can be viewed as effective degrees of freedom. Thus, in cases where the spatiotemporal dynamics are governed by only a few degrees of freedom, the first few modes already capture most of the signal content, i.e., they contain most of the 'energy' which is in the system.

3. Local fluctuations and critical behaviour

Catalytic CO oxidation on noble metal surfaces (Pt, Pd, Ir) proceeds via the Langmuir–Hinshelwood (LH) mechanism comprising the following steps [33]:

$$CO + * \leftrightarrow CO_{ad}$$
$$O_2 + 2* \rightarrow 2O_{ad}$$
$$CO_{ad} + O_{ad} \rightarrow CO_2 + 2*$$

with * denoting a vacant adsorption site.

Catalytic CO oxidation on a structurally stable Pt surface exhibits two branches of the kinetics as shown schematically in figure 2. On the active branch the surface is predominantly

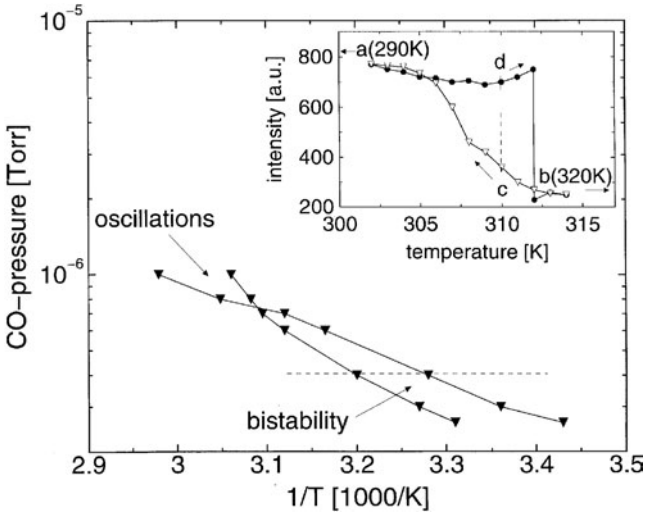

Figure 3. Bifurcation diagram for catalytic CO oxidation on a [100]-oriented Pt tip at $p_{O_2} = 4.0 \times 10^{-4}$ Torr. In the region enclosed by the two boundary lines the system is bistable below the crossing point (critical point) and oscillatory above the crossing point of the two lines. To the left of this region, the system is in a stable oxygen-covered state, to the right in a stable CO-covered state. The inset shows the hysteresis in local FEM brightness (20×20 Å^2) for an area close to (110) upon cyclic variation of T: filled triangles—heating, empty triangles—cooling (from [23]).

oxygen covered so that CO can still adsorb and react. On the inactive branch a high CO coverage inhibits O_2 adsorption and hence poisons the reaction. In the bistable regime the two stable branches coexist leading to a hysteresis upon variation of the bifurcation parameter.

The bifurcation diagram of the Pt tip used in our experiments is displayed in figure 3 [21, 31]. The system is bistable in a broad parameter range giving rise to a hysteresis in local FEM brightness upon variation of a bifurcation parameter (usually the temperature). Remarkably, although the various orientations on the tip differ quite strongly in their reactivity (due to different oxygen sticking coefficients), fast CO diffusion apparently ties the different facets together so that the tip behaves as one dynamical system during such transitions. At the left- and right-hand boundaries of the bistability range the whole tip becomes CO covered and oxygen covered, respectively.

Already when the surface is covered by only one adsorbate we observe local brightness fluctuations, which arise from local fluctuation in the particle density as adsorbed particles diffuse in and out of a particular area chosen for observation. In fact, the analysis of these fluctuations via the autocorrelation function has been used as a very successful method for the determination of surface diffusion constants [34].

Under reaction conditions we observe brightness fluctuations that arise both from surface diffusion and from the additional influence of the surface reaction. In the bistable regime of the reaction we observe strong brightness fluctuations whose amplitude and characteristics vary depending on the selected surface orientation. First, we neglect completely the aspect of spatial coupling and focus on the local fluctuations in an area of $\approx 20 \times 20$ Å^2 corresponding to a few hundred adsorbed particles. In these fluctuations bright areas represent the inactive branch where the surface is CO covered and dark areas the active branch of the reaction where the surface is

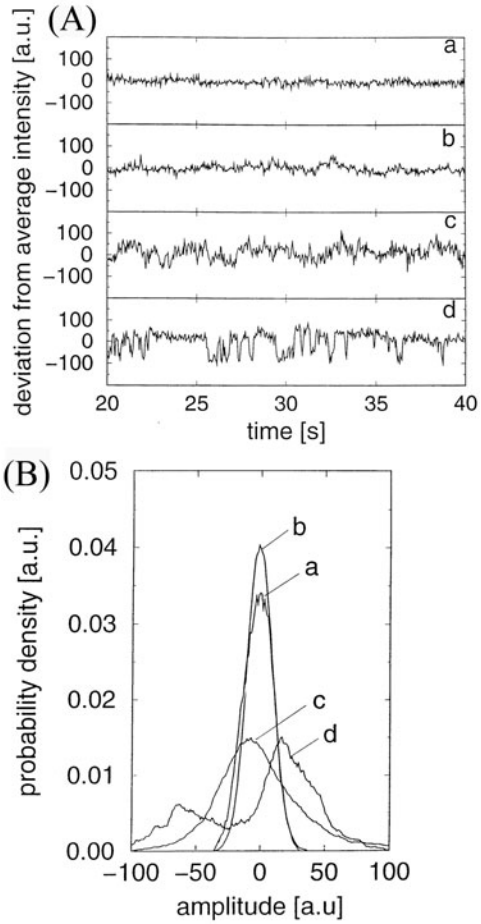

Figure 4. Fluctuations in catalytic CO oxidation on Pt(110) under different reaction conditions (from [23]). (A) Time series of the local (20×20 Å^2) FEM brightness in an area close to (110). The data were recorded at different points marked on the hysteresis loop in the inset of figure 3. (B) Probability distributions corresponding to the time series shown in (A).

predominantly oxygen covered.

The times series in figure 4(A) were recorded from such a 20×20 Å^2 area in the vicinity of Pt(110) [23]. We first take a look at the dependence of the brightness fluctuations on the reaction conditions. The different time series displayed in figure 4(A) correspond to a CO-covered (inactive) and an oxygen-covered (active) surface in the monostable range (a, b in the inset of figure 3) and to states in the bistable range (c, d in the inset of figure 3) of the reaction. From the time series, probability distributions of the intensity fluctuations have been constructed (figure 4(B)). In the monostable ranges (a, b) relatively narrow distributions of roughly Gaussian shape are found, but in the bistable range the distributions become rather broad. On the active branch, the peak just broadens and becomes slightly asymmetric (c), but on the inactive branch (d) the distribution actually becomes bimodal. This bimodal distribution is evidence for fluctuation-(noise-) induced transitions between the two 'stable' states, where the system is typically in one of these states, and spends comparatively little time in transition between them.

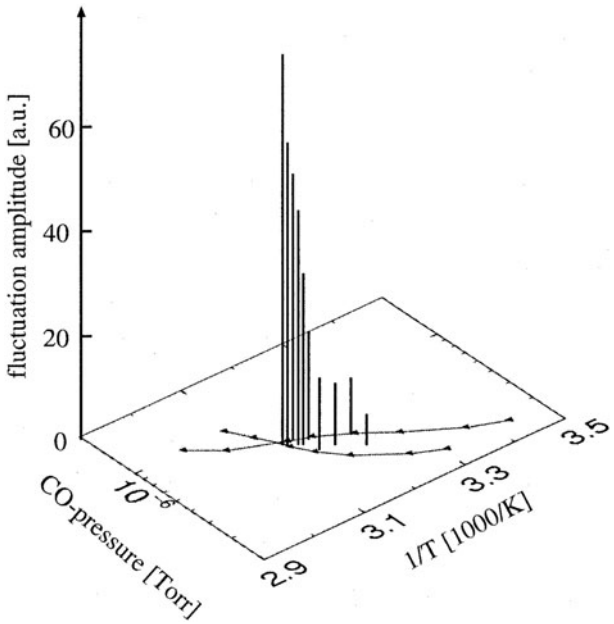

Figure 5. Critical behaviour of fluctuations. Shown is the increase in the average amplitude of the local FEM brightness fluctuations on a Pt(112) facet with decreasing distance to the critical point giving by the crossing of the two boundary lines of the bistability range (from [25]).

Of decisive influence for the amplitude of the fluctuations is the proximity to the point (C) where the two boundaries cross in figure 3. This point, which terminates the bistable range of the reaction is not a cusp point because an oscillatory range opens up on the other side as the two boundaries cross at C. As demonstrated by figure 5 with data taken from the Pt(112) facet upon approaching C the amplitude of the fluctuations increases drastically [25]. The amplitude of the fluctuations seems to diverge at C, which plays the role of a critical point. Point C itself is not accessible experimentally because the system is so unstable there that it rapidly ends up either on the inactive or active branch of the reaction. The behaviour of the amplitude of the fluctuations suggests a close analogy to the behaviour of an equilibrium phase transition near a critical point. This analogy obtains further support from simulations summarized in the following section. As supported by simulations point C plays a role similar to that of a critical point in an equilibrium phase transition.

4. Simulations

A method which naturally is well suited for describing the fluctuations or internal noise caused by the stochastic nature of the elementary process is MC simulation. Numerous MC simulations of catalytic CO oxidation have already been carried out mostly based on the simplified Ziff–Gulari–Barshed (ZGB) scheme [35, 36]. An analysis of the fluctuations in this system has been conducted by Fichthorn *et al* [36]. The ZGB scheme, which is favoured by many groups in statistical physics, is not suitable for simulating real experiments because it contains an unrealistic poisoning of the surface by adsorbed oxygen and it neglects CO diffusion, CO desorption and all energetic interactions between the adparticles. Improved models have, of course, been suggested

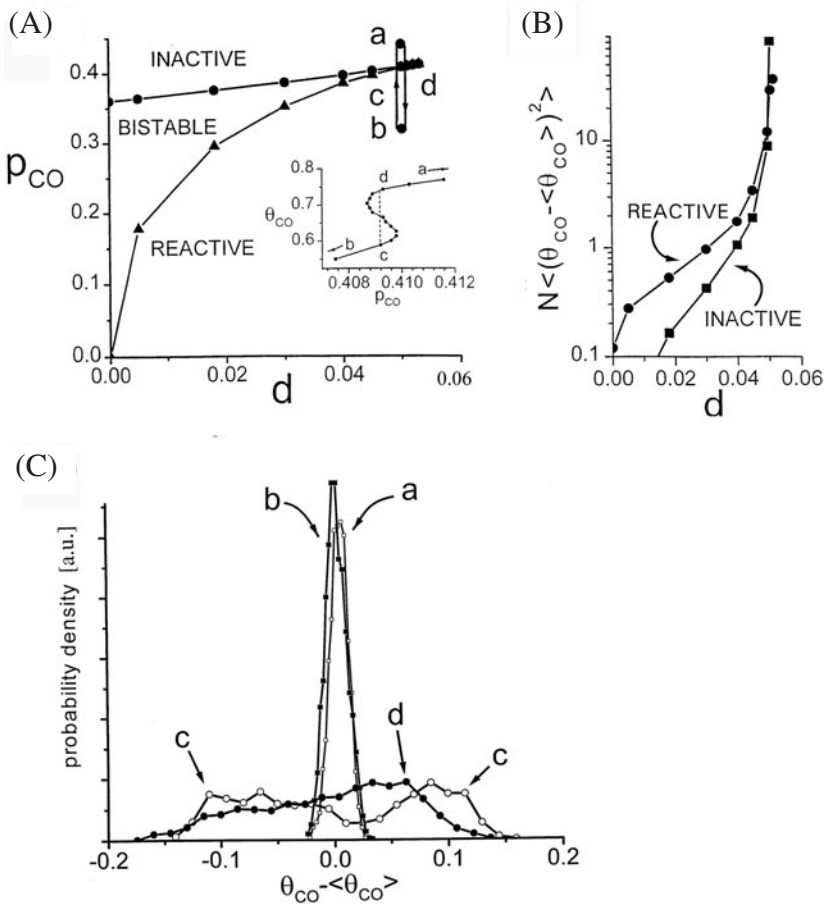

Figure 6. Simulations of fluctuations on a small Pt facet with a hybrid model (see text) (from [23]). (A) Simulated bifurcation diagram showing the bistability region. The inset shows a hysteresis in θ_{CO} for fixed $d = 0.05$. In the experiment (figures 3, 4) the temperature corresponds to d. (B) Amplitude of fluctuations in θ_{CO} for the reactive and inactive branches at the midpoint of the bistability region. N denotes the system size in number of sites. (C) Probability distributions for θ_{CO} on a 60×60 lattice with $d = 0.050$ for points marked on the hysteresis loop in (A).

by numerous authors but the essential drawback of all these lattice gas models is the inability to model realistically the very fast surface diffusion of CO [37]. In the following a hybrid model developed by Evans *et al* [23, 25, 27] is presented aimed at properly taking this aspect into account.

The basis of the model is the three-step scheme of the LH mechanism presented above. The (100) and (110) orientations are known to undergo an adsorbate-induced surface phase transition which has been identified as driving for oscillatory behaviour of catalytic CO oxidation on Pt surfaces [16, 17]. The phase transitions are activated. At our measuring temperature around 300 K the kinetics of structural rearrangements should be slow compared to the time scale of fluctuations so that we are justified in neglecting a restructuring of the surface. All catalytic

reactions are of course known to cause substrate modifications and for longer times (minutes to hours) such changes, which will show up as drifts in the experimental data, have to be taken into account [38]. For the short observation times used here such effects should be small.

At 300 K oxygen is practically immobile on the surface whereas CO is highly mobile. The different mobilities of CO(ads) and O(ads) are taken into account in a hybrid model. Only adsorbed oxygen is described by a full lattice gas model, while adsorbed CO is treated as an MF variable, i.e. it is assumed that CO diffuses infinitely fast occupying all available sites with the same probability [27]. The experimental observation that oxygen on a Pt(111) surface forms a (2×2) superlattice is also part of the model encoded in an eight-site rule (see below) [39]. The following rules have been set up:

(i) CO(gas) adsorption onto single empty sites at rate p_{CO}. CO(ads) hops very rapidly to other empty sites on the surface, so it is assumed randomly distributed on sites not occupied by O(ads) (neglecting CO–CO and CO–O interactions). CO(ads) also desorbs from the surface at rate d.

(ii) O_2(gas) adsorption dissociatively at diagonal nearest-neighbour (NN) empty sites at rate p_{O_2}, *provided* that the *additional* six sites adjacent to these are not occupied by O(ads). This 'eight-site rule' reflects the very strong NN O(ads)–O(ads) repulsions. O(ads) is also immobile and cannot desorb, so O(ads) never occupies adjacent sites.

(iii) Each adjacent pair of CO(ads) and O(ads) can react at rate k to form CO_2(gas).

Simulations have been conducted for a square 60×60 lattice with periodic boundary conditions and setting $p_{O_2} + p_{CO} = 1$. The results are reproduced in figure 6. To compare the results with the experiments the CO desorption constant d has been used as the bifurcation parameter because CO desorption as the most strongly activated surface process will react highly sensitively to variations of the temperature. The parameter d in the simulations therefore corresponds to the temperature in experimental data. Figure 6(A) shows that the width of the bistable region shrinks with increasing d (temperature) vanishing in a cusp point. The amplitude of the fluctuations displayed in (B) diverges towards the cusp point, which therefore plays the role of a critical point. Upon variation of p_{CO} one obtains a hysteresis in the CO coverage shown in the inset of figure 6(A). Fluctuations in the CO and in the oxygen coverage are typically anticorrelated due to fast reaction between the two adsorbates. For comparison with the experiment the probability distribution of the fluctuations has been determined for different states of reactivity as indicated in the hysteresis in the inset of figure 6(A). The narrow amplitude distribution in the monostable regime and the broad bimodal distributions in the bistable regime of the reaction seen in the experiment (see figure 4(B)) are well reproduced by the simulation. Fluctuation-induced transitions indicated by bimodal distributions are only observed for small lattice sizes. For a 60×60 site system the transition from monomodal to bimodal distribution occurs for $d \approx 0.045$, but for a 30×60 lattice this transition already occurs at $d \approx 0.040$. Qualitatively the same trend due to size effects can be observed with the four symmetry equivalent (112) orientations indicated in figure 1(C), which differ in size [26].

The behaviour of the amplitude of the fluctuations towards the critical point is similar to that of an equilibrium phase transition near the critical point. Further support for this analogy comes from the correlation time, which also diverges towards the critical point as demonstrated by figure 7 [25]. This increase in the correlation time is generally known as critical slowing down.

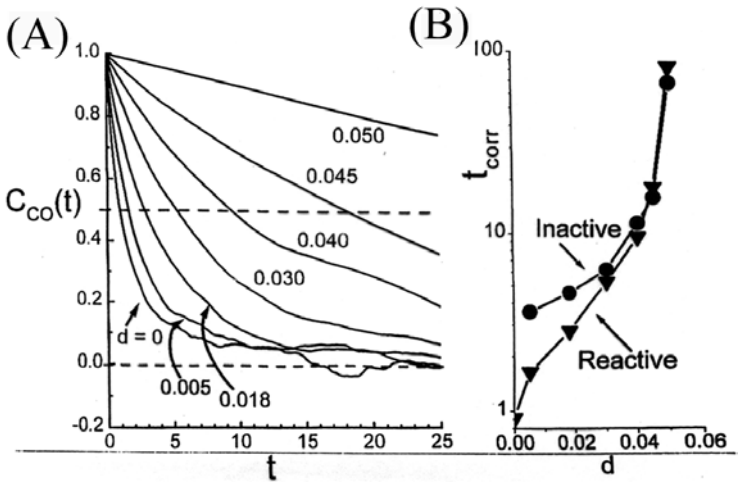

Figure 7. Simulated behaviour of the correlation time in fluctuations upon approaching the critical (cusp) point ($d \rightarrow d_c$) of the bifurcation diagram (see figure 6(A)) (from [25]). (A) Autocorrelation function of the CO coverage $C_{CO}(t)$ versus t for various d (shown); (B) the corresponding increase in t_{corr}, defined as time for the correlation to decay to 50% of the initial value. Shown are the data for the inactive and reactive branches as $d \rightarrow d_c$.

5. Spatial correlations and coupling effects

The Pt tip is dynamically a very complex system because the surface consists of facets of different sizes and reactivities coupled together via CO diffusion. In contrast to CO, for which sticking is almost independent of the surface orientation and close to one, the sticking coefficient of oxygen is highly structure sensitive on Pt surfaces [40]. Variations over several orders of magnitude have been reported in single-crystal studies ranging from 10^{-4} for the quasi-hexagonal reconstructed Pt(100) surface to $s_{O_2} \approx 0.6$ for Pt(210) [40, 41]. The differences may be smaller on a Pt tip due to the smallness of the facets but one still has a strongly varying catalytic activity for the various orientations of the Pt tip. The surface diffusion of CO is known to be slowed down considerably at atomic steps (depending on step orientation) [42] and hence we can expect that the atomic steps and structurally rough areas which terminate the flat regions of the low-index facets will make communication between different facets more difficult. A distinction between coupling effects within a facet (intrafacet coupling) and coupling between facets (interfacet coupling) therefore appears to be appropriate.

From the digitized video images we can extract local time series at two arbitrary points of the Pt tip. By varying the distance between two such time series measured in 20×20 Å^2 windows we obtain the spatial two-point correlation function. We first take a look at the intrafacet correlation under varying reaction conditions displayed in figure 8(B) for one of the large Pt(111) facets of the Pt tip [22]. On the CO-poisoned surface in the monostable range we find only very short-range correlations limited to <20 Å (curve a). The correlation is practically identical to that in pure CO, i.e., the reaction plays no role and the spatial correlation is entirely determined by CO diffusion alone. On the active branch in the monostable range (curve d) the correlation is practically the same as on the inactive branch despite the fact that the surface is oxygen covered under these conditions. We observe far-reaching correlations in the bistable range of the reaction

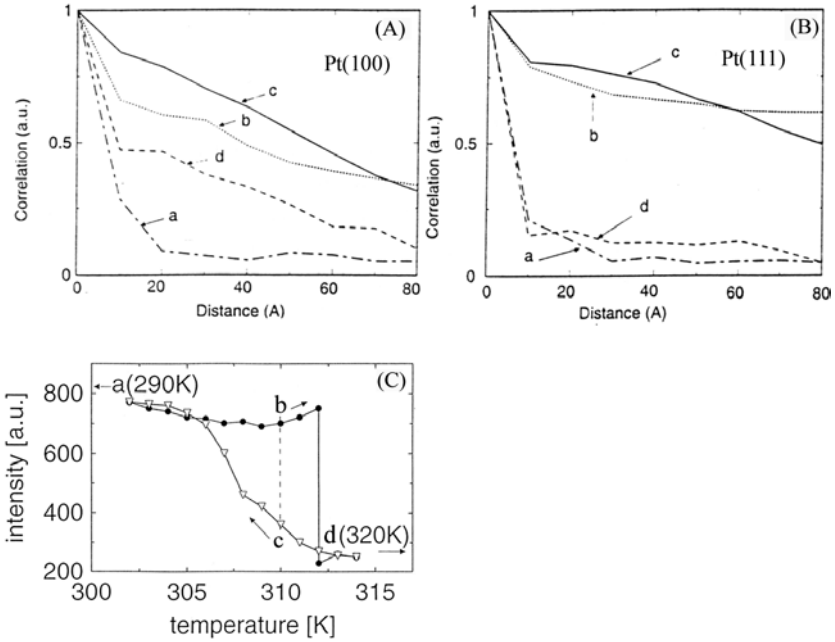

Figure 8. Comparison of the spatial correlation (two-point correlation function) for fluctuations on a Pt(111) facet and on a Pt(100) facet. The different curves represent different reaction conditions as indicated in the hysteresis measurement. The distance zero refers to the left-hand edge of the facet (from [22]).

for both the active (curve c) and for the inactive branch of the reaction (curve b). In both cases the spatial correlation remains high over the entire range of the Pt(111) facet. A high degree of spatial correlation in fluctuation-induced transitions has also been found on all other facets investigated. In a POD analysis over the area of such facets this synchronized behaviour is reflected by the dominance of one mode [24]. The first mode alone typically already captures about 70–90% of the total energy.

When we study under identical p, T-parameters the fluctuations on different facets we see that their fluctuation behaviour is quite different. This is demonstrated in figure 9, showing fluctuations which have been recorded simultaneously on two different orientations, Pt(111) and Pt(100), at varying reaction conditions [22]. The different characteristics are also reflected in the spatial correlation functions displayed in figure 8. Both orientations exhibit very short-range correlations on the inactive monostable regime (curves a) and both show long-range correlations on the active branch in the bistable range (curves c). On Pt(100), however, the correlation of the active monostable branch (curve d) is much higher than on Pt(111) over a large part of the region. The similarity between the correlation functions for the active and inactive branches in the bistable range (curves b and c) is far less pronounced on Pt(100) than on Pt(111).

The differences in the fluctuation behaviour of different facets can be rationalized if we take into account that despite identical p, T-parameters different facets can be in different dynamic regimes due to their differences in reactivity. Coupling via CO diffusion is apparently not strong enough to synchronize the fluctuations on different facets, which retain their local character. We can see that an atomic step already causes a significant loss in spatial correlation when we follow the spatial correlation beyond the boundary of a facet. This was done for a Pt(112)

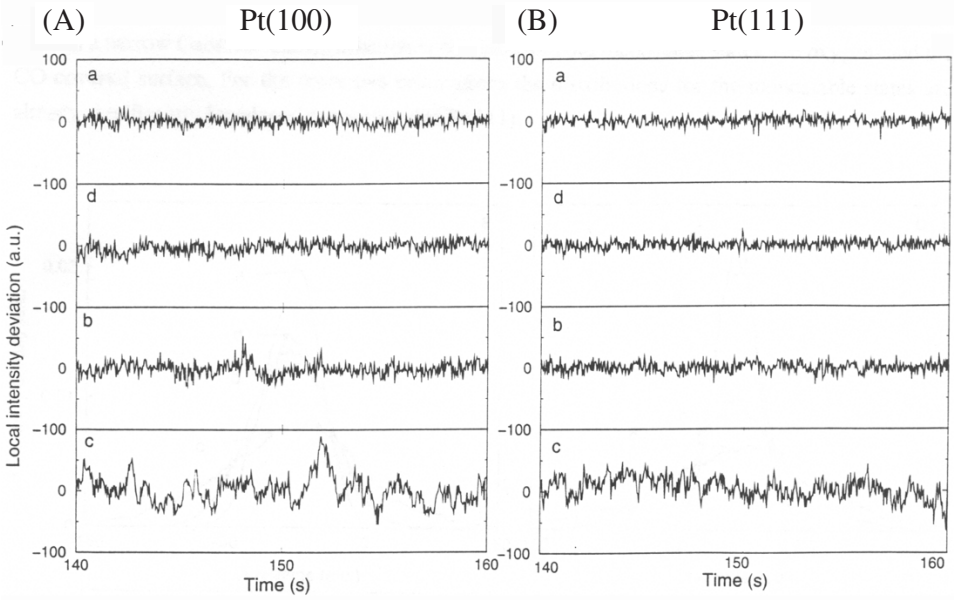

Figure 9. Local fluctuations on Pt(100) and Pt(111) demonstrating the absence of synchronization (from [22]). The letters a, b, c and d refer to different reaction conditions indicated in figure 8(C). The time series on the two facets were recorded simultaneously.

facet where, as demonstrated by figure 1(D), the bright ring surrounding the central dark area represents an atomic step terminating the (211) facet [25]. The atomically flat (211) facet itself that is symmetry equivalent to Pt(112) is imaged as dark area. As shown in figure 10 at the position of the step marked with an arrow in the plot the spatial correlation function starts to decay quite steeply. The different curves in this diagram represent time series recorded under different reaction conditions with curves h and i being taken close to the critical point in the bifurcation diagram of figure 3 and curve c recorded under conditions further away from this point. The spatial correlation is seen to increase with decreasing distance from the critical point and this is a general tendency found also in other analyses.

The general conclusion which could be drawn from the correlation studies was that fluctuations are well correlated within one single facet but typically no correlations exist between fluctuations on different facets except for conditions very close to the critical point. The conclusion that interfacet coupling via CO diffusion is negligible would still be wrong. The fact that all facet orientations at the boundaries of the bistable range (see figure 3) undergo simultaneously the transition to a completely CO- or oxygen-covered surface shows that efficient coupling via CO diffusion has to exist tying the reactivities of the various orientations together. Apparently, inside the bistable range coupling via CO diffusion is present but only up to the degree that the individual facets can retain their local fluctuation characteristics. At the boundaries of the bistable range probably in a kind of avalanche effect the transition of a few orientations to one of the nonstable branches of the reaction triggers the transformation of the whole tip. This would imply that the boundaries in the bifurcation diagram of figure 3 depend on the shape of the Pt tip and this is what is observed experimentally [25, 31].

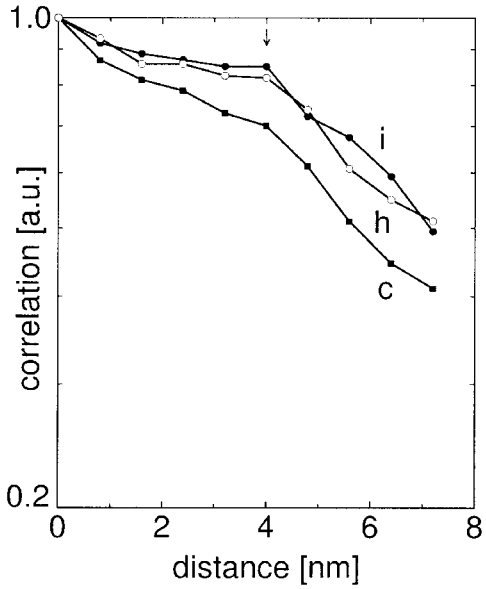

Figure 10. Influence of atomic steps on the spatial correlation of fluctuations. Shown is the spatial (two-point) correlation of fluctuations on the (112) facet as determined from local (0.8×0.8 nm^2) time series. The letters refer to different reaction conditions (see text). The distance zero refers to the left-hand edge of the facet (from [25]).

In our fluctuation studies on the Pt tip we have so far not observed any propagating reaction fronts as they are characteristic for catalytic CO oxidation on Pt single-crystal surfaces [16, 17]. If we take a typical front velocity of 1 μm s^{-1} and calculate the time it would take for such a front to traverse a facet of 100 Å diameter we obtain 1/100 s. This time is much shorter than the time resolution of conventional video cameras of 20 ms with which nearly all measurements in this study have been carried out. The high spatial correlation we see for fluctuations within a single facet might thus not be caused by a true synchronized behaviour but just is due to reaction fronts, which sweep across the area of a facet within a time too short to be detected by conventional video cameras. Experiments with a fast camera to answer this question are planned.

A full dynamical modelling of catalytic CO oxidation including all facets of the Pt tip and all structural influences is clearly far beyond the scope of present simulation techniques. Pavlenko *et al* [28] presented a model aimed at studying the coupling effects between just two neighbouring facets with bistable kinetics. The simulation is based on the hybrid model but while infinitely fast CO diffusion is assumed to occur within each facet the coupling between facets should take place via a finite CO hopping rate h. The slowing down of CO diffusion at the edge of a facet is expected to be a natural consequence of the enhanced surface roughness there. The two facets are of equal size but exhibit different reactivities expressed here as different oxygen sticking coefficients S_O^1 and S_O^2. As demonstrated by figure 11(A) coupling the two bistable systems leads to complex multistability on each of the facets. For the case of medium coupling shown in this figure the large-amplitude fluctuations are clearly synchronized.

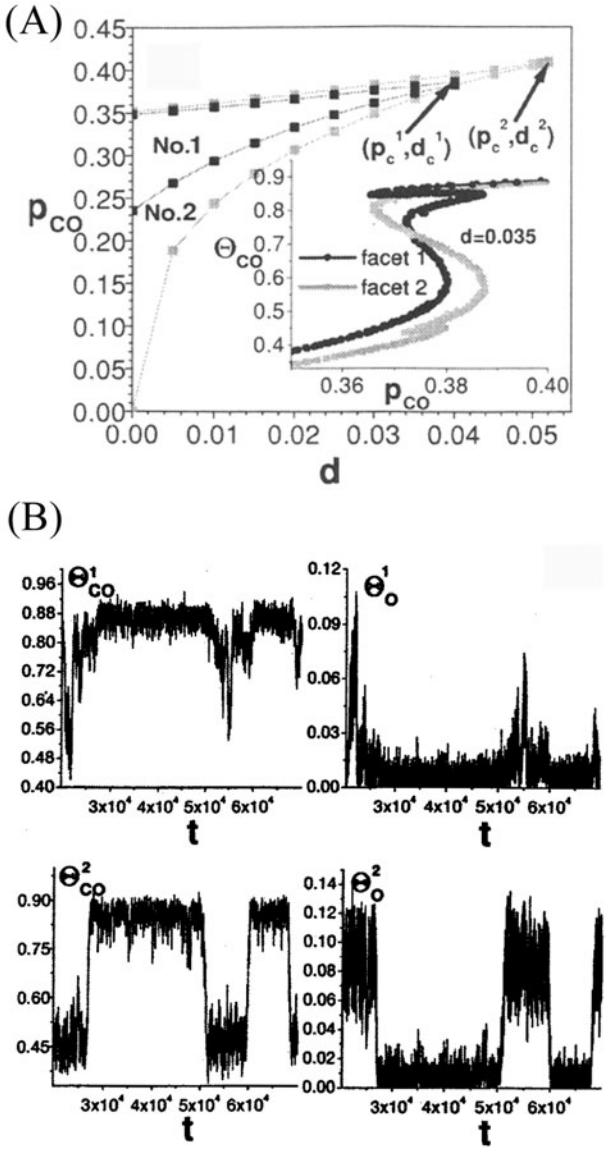

Figure 11. Simulated fluctuations on two facets coupled via CO diffusion with medium coupling strength ($h = 0.018$) (from [28]). (A) Bifurcation diagram showing the bistability ranges of the two facets with the partial pressure of CO, p_{CO}, and the CO desorption constant, d, as bifurcation parameters. The latter represents the temperature in the experiment. The inset shows the stationary solution θ_{CO} for both facets with fixed $d = 0.035$ as p_{CO} is varied. (B) Fluctuations in the CO and in the oxygen coverage on both facets at reaction conditions close to the cusp point in (A).

6. Conclusions and outlook

It has been shown that catalytic surface reactions on a FET are well suited for studying internal fluctuations in a chemical reaction system. Effects predicted by theory like fluctuation-induced transitions in a bistable system could be verified experimentally in catalytic CO oxidation on

a Pt tip. A particular appealing feature is that the reaction-induced fluctuations near a critical point exhibit a behaviour very similar to that of an equilibrium phase transition. The amplitude of the fluctuations increases drastically upon approaching the critical point and—this has so far only been seen in simulations—the correlation time diverges indicating critical slowing down. The Pt tip is a dynamically a complex system consisting of different surface orientations with different reactivities coupled via surface diffusion of CO. Within each facet the fluctuations are spatially well correlated reflecting efficient synchronization via CO diffusion. Quite in contrast no correlations are found between fluctuations on different facets—a fact attributed to (i) restricted CO mobility at the edges of the facets and (ii) different catalytic activities of the facets. Each facet therefore retains its own fluctuation characteristics unless at the boundaries of the bistable range where the whole tip undergoes the transition to a CO/oxygen-covered state.

For a realistic simulation of CO oxidation on small Pt facets a hybrid model was developed combining MC simulations with MF modelling. The model, which assumes an infinite mobility of adsorbed CO, was capable of reproducing many of the characteristic features of the experiment. At present the experiment is strongly limited by the relatively slow rate (20 ms/frame) of conventional video cameras. The question of whether fast travelling reaction fronts are responsible for synchronization within a facet could be answered by experiments with a fast camera. Such experiments, which are feasible (1000 frames s^{-1} can easily be achieved), will expand the time scale of observable processes and are expected to lead to the discovery of new phenomena. With the development of nanostructured systems fluctuations will become an issue of great practical importance because such effects will dominate the reactivities of these systems.

References

[1] van Kampen N G 1987 *Stochastic Processes in Physics and Chemistry* (Amsterdam: North-Holland)
[2] Gardiner C W 1983 *Handbook of Stochastic Methods for Physics, Chemistry and the Natural Sciences* (Berlin: Springer)
[3] Malchow H and Schimansky-Geier L 1985 *Noise and Diffusion in Bistable Nonequilibrium Systems* (Berlin: Teubner)
Ebeling W and Schimansky-Geier L 1979 *Physica* A **98** 587
[4] Mikhailov A S and Loskutov A Yu 1996 *Foundations of Synergetics* vol 2, 2nd edn (Berlin: Springer)
[5] Kondepudi D and Progogine I 1998 *Modern Thermodynamics* (New York: Wiley)
[6] Horsthemke W and Lefever R 1984 *Noise-Induced Transitions* (Berlin: Springer)
[7] Hanggi P *et al* 1990 *Rev. Mod. Phys.* **62** 251
[8] Vlad M O and Ross J 1994 *J. Chem. Phys.* **100** 7268
Vlad M O and Ross J 1994 *J. Chem. Phys.* **100** 7279
Vlad M O and Ross J 1994 *J. Chem. Phys.* **100** 7295
Mikhailov A S 1981 *Z. Phys.* B **41** 277
[9] Xu X-H and Yeung E S 1997 *Science* **275** 1106
[10] Kadar S, Wang J and Showalter K 1998 *Nature* **391** 770
[11] Satterfield C N 1980 *Heterogeneous Catalysis in Practice* (New York: McGraw-Hill)
[12] Zhdanov V P and Kasemo B 1998 *Surf. Sci.* **405** 27
Zhdanov V P and Kasemo B 1998 *Surf. Sci.* **412/413** 527
[13] Zhdanov V P and Kasemo B 2000 *Surf. Sci. Rep.* **39** 25
[14] Hildebrand M and Mikhailov A S 1996 *J. Chem. Phys.* **100** 19089
[15] Müller E W and Tsong T T 1969 *Field Ion Microscopy* (New York: Elsevier)
[16] Eiswirth M and Ertl G 1994 *Chemical Waves and Patterns* ed R Kapral and K Showalter (Dordrecht: Kluwer)

[17] Imbihl R and Ertl G 1995 *Chem. Rev.* **95** 697
[18] van Tol M F H, Gielbert A and Nieuwenhuys B E 1992 *Catal. Lett.* **16** 297
[19] Gorodetskii V, Drachsel W and Block J H 1993 *Catal. Lett.* **19** 223
[20] Gorodetskii V, Lauterbach J, Rotermund H-H, Block J H and Ertl G 1994 *Nature* **370** 276
[21] Suchorski Y, Beben J and Imbihl R 1998 *Surf. Sci.* **405** L477
[22] Suchorski Y, Beben J and Imbihl R 1998 *Prog. Surf. Sci.* **59** 343
[23] Suchorski Y, Beben J, James E W, Evans J W and Imbihl R 1999 *Phys. Rev. Lett.* **82** 1907
[24] Suchorski Y, Beben J and Imbihl R 2000 *Surf. Sci.* **454–456** 331
[25] Suchorski Y, Beben J, James E W, Liu D-J, Evans J W and Imbihl R 2001 *Phys. Rev.* B **63** 165417
[26] Suchorski Y, Beben J and Imbihl R, in preparation
[27] Liu D-J and Evans J W 2002 *J. Chem. Phys.* **117** 7319
[28] Pavlenko N, Evans J W, Liu D-J and Imbihl R 2001 *Phys. Rev.* E **65** 16121
[29] Liu D-J, Pavlenko N and Evans J W 2003 submitted
[30] Miller M K and Smith G D W 1989 *Atom Probe Microanalysis* (Pittsburgh, PA: Materials Research Society)
[31] Suchorski Y, Imbihl R and Medvedev V K 1998 *Surf. Sci.* **401** 392
[32] Lumley J L 1970 *Stochastic Tools in Turbulence* (New York: Academic)
[33] Engel T and Ertl G 1979 *Adv. Catal.* **28** 1
[34] Gomer R 1990 *Rep. Prog. Phys.* **53** 917
[35] Ziff R M, Gulari E and Barshad Y 1986 *Phys. Rev. Lett.* **56** 2553
[36] Fichthorn K, Gulari E and Ziff R M 1989 *Phys. Rev. Lett.* **63** 1527
[37] Evans J W 1991 *Langmuir* **7** 2514
[38] Imbihl R 1992 *Mod. Phys. Lett.* B **6** 493
[39] Brundle C R, Behm R J and Barker J A 1984 *J. Vac. Sci. Technol.* A **2** 1038
Chang S-L and Thiel P A 1987 *Phys. Rev. Lett.* **59** 296
[40] Sander M, Imbihl R and Ertl G 1992 *J. Chem. Phys.* **97** 5193
[41] Guo X-C, Bradley J M, Hopkinson A and King D A 1994 *Surf. Sci.* **310** 163
[42] Tammaro M, Evans J W, Rastomjee C S, Swiech W, Bradshaw A M and Imbihl R 1998 *Surf. Sci.* **407** 162